Mechanisms of Acid Resistance in *Escherichia coli*

Usheer Kanjee[1,2] and Walid A. Houry[2]

[1]Department of Immunology and Infectious Diseases, Harvard School of Public Health, Boston, Massachusetts 02115; email: ukanjee@hsph.harvard.edu

[2]Department of Biochemistry, University of Toronto, Toronto, Ontario M5S 1A8, Canada; email: walid.houry@utoronto.ca

Annu. Rev. Microbiol. 2013. 67:65–81

First published online as a Review in Advance on May 20, 2013

The *Annual Review of Microbiology* is online at micro.annualreviews.org

This article's doi: 10.1146/annurev-micro-092412-155708

Keywords

pH homeostasis, amino acid decarboxylase, stringent response, ppGpp, amino acid transporter

Abstract

Adaptation to acid stress is an important factor in the transmission of intestinal microbes. The enterobacterium *Escherichia coli* uses a range of physiological, metabolic, and proton-consuming acid resistance mechanisms in order to survive acid stresses as low as pH 2.0. The physiological adaptations include membrane modifications and outer membrane porins to reduce proton influx and periplasmic and cytoplasmic chaperones to manage the effects of acid damage. The metabolic acid resistance systems couple proton efflux to energy generation via select components of the electron transport chain, including cytochrome *bo* oxidase, NADH dehydrogenase I, NADH dehydrogenase II, and succinate dehydrogenase. Under anaerobic conditions the formate hydrogen lyase complex catalyzes conversion of cytoplasmic protons to hydrogen gas. Finally, each major proton-consuming acid resistance system has a pyridoxal-5′-phosphate-dependent amino acid decarboxylase that catalyzes proton-dependent decarboxylation of a substrate amino acid to product and CO_2, and an inner membrane antiporter that exchanges external substrate for internal product.

Contents

ESCHERICHIA COLI ACID STRESS RESPONSE

Enteric bacteria are found naturally in the digestive tracts of mammals and include many species of commensal and pathogenic organisms, which typically grow best under neutral pH conditions. During passage through the human digestive tract, enteric bacteria must first survive the extremely acidic stomach, where a pH between 1.5 and 3.0 acts as a potent barrier against microbial infection (13, 83). Most pathogenic bacteria require a large infectious dose (e.g., *Vibrio cholerae* requires $\sim 10^9$ organisms) (33, 54, 64) in order to ensure that some organisms survive passage through the stomach. Remarkably, infectious enterohemmorhagic *Escherichia coli* requires a substantially lower infectious dose ($\sim 10^2$ organisms), and this has been attributed to the robust survival of this bacteria at low pH (33, 54). Under laboratory conditions, *E. coli* is capable of surviving a pH stress of 2.0 for several hours (13, 53, 54), underscoring the potent ability of this organism to withstand acidic conditions. In addition, some bacteria, such as *Helicobacter pylori*, are adapted to grow in the stomach despite the low pH (56). After passage through the stomach, bacteria enter the relatively neutral or basic small intestine (60). However, the environment of the intestine is rich in carbohydrates and low in oxygen, leading to high levels of fermentation and the consequent production of short-chain fatty acids (SCFAs) such as formic, acetic, propionic, and lactic acids (38, 58, 60). SCFAs cross the cell membrane in an uncharged state and subsequently dissociate in the cytoplasm, resulting in a lowering of the internal pH. Hence, bacterial cells face acid stress even in the intestine.

To counteract acid stresses, cells utilize a combination of passive and active acid resistance (AR) systems. The passive system of acid resistance arises owing to the buffering capacity of the amino acids, proteins, polyamines, polyphosphate, and inorganic phosphate present in the cytoplasm that together contribute between 50 and 200 mM buffering capacity per pH unit (77). The active systems can be divided into physiological, metabolic, and proton-consuming systems. The regulation and function of bacterial acid stress response systems have been reviewed previously (27, 50, 77, 94). Here, we initially provide an overview of the physiological and metabolic systems but then focus mainly on the recent structural insights into the proton-consuming AR systems of the model enteric bacterium *E. coli*.

SCFA: short chain fatty acid

Extreme acid stress: refers to external pH conditions within the range of 2.0 to 3.0

PHYSIOLOGICAL ADAPTATIONS TO ACID STRESS

There are numerous definitions of what constitutes acid stress, but for this review we use the following terms: Extreme acid stress refers to external pH conditions within the range of 2.0 to 3.0;

mild acid stress refers to external pH conditions within the range of 4.0 to 5.0. The first sites of acid damage in *E. coli* are the outer membrane and the periplasm, as these are in direct contact with the external environment. *E. coli* can reduce the influx of protons by changing the composition of the membranes to decrease membrane fluidity and thus permeability to protons. This is accomplished by reducing the concentration of unsaturated lipids (93) and increasing the concentration of cyclopropane fatty acids through the action of cyclopropane fatty acyl phospholipid synthase (8, 14) (**Figure 1*a***). Furthermore, proton influx can be reduced by blocking the outer membrane porins (OMPs) by the binding of polyphosphate or cadaverine to the OMPs (19, 68, 71) (**Figure 1*b***).

The periplasm also has two chaperone proteins, HdeA and HdeB (28), that are transcribed as part of the GadE-dependent acid fitness island (57, 69). HdeA and HdeB are small α-helical proteins that are dimeric at neutral pH but dissociate into partially unfolded monomers at low pH and bind to acid-denatured substrate proteins (28, 48) (**Figure 1*c***). As the pH increases, HdeA and HdeB slowly release substrate proteins in a refolding-competent conformation (80). This single binding-and-release cycle is an important adaptation because proteins in the periplasm are not able to access the ATP-dependent chaperone systems such as the cytoplasmic GroEL/ES or DnaK/DnaJ/GrpE systems (40).

Although *E. coli* has numerous cytoplasmic chaperones that operate efficiently during stresses, such as heat shock, to date only the Hsp31 chaperone (**Figure 1*d***) has been implicated in acid stress (61). Homodimeric Hsp31 functions as a holdase: It binds to and stabilizes unfolded intermediates until the stress is relieved and then allows the proteins to refold either spontaneously or through the ATP-dependent chaperone systems (65). In addition to Hsp31, various low-molecular-weight proteins have been implicated in cell envelope stress and acid stress; however, the molecular basis for the action of these proteins is still under investigation (39, 52). Apart from protein chaperones, the DNA-binding Dps (DNA-binding protein from starved cells) protein contributes to extreme acid stress survival by binding to and protecting DNA (15) (**Figure 1*e***). Dps oligomerizes to form a dodecameric cage-like structure with a hollow interior that sequesters Fe^{2+} ions (34), thus reducing the formation of damaging hydroxyl free radicals via the Fenton reaction (95).

Mild acid stress: refers to external pH conditions within the range of 4.0 to 5.0

OMP: outer membrane porin

Proton motive force (PMF): the inner membrane proton gradient used to power ATP generation and active transport processes

METABOLIC RESPONSES TO ACID STRESS

Global transcription analysis of *E. coli* growth during either aerobic or anaerobic conditions under mild acid stress (pH 5.0–5.7) has revealed metabolic changes that provide protection against low pH (38, 58, 77). Among these changes are an induction of stress response systems, including the periplasmic stress response and the oxidative stress response (under aerobic conditions). Interestingly, there is an increase in genes involved in transport and metabolism of secondary carbon sources. These carbon sources include sugars (ribose, arabinose, fuculose) and sugar derivatives (galactitol, sorbitol, melibiose, mannitol, gluconate) that produce fewer acids upon metabolism compared with glucose, which is beneficial to an acid-stressed cell.

During aerobic growth under mild acid stress, there is an upregulation of selected components of the electron transport chain, including cytochrome *bo* oxidase (CBO) (*cyo* genes), NADH dehydrogenase II (NDH-II) (*ndh* genes), succinate dehydrogenase (SDH) (*sdh* genes), and NADH dehydrogenase I (NDH-I) (*nuo* genes) (58, 77) (**Figure 2**). Under normal growth conditions these systems are involved in generating the proton motive force (PMF) by coupling metabolic redox reactions (such as oxidation of NADH to NAD) with the direct or indirect export of protons from the cell. The heme-copper CBO complex accepts electrons from ubiquinol-8 (a quinone) and catalyzes the conversion of cytoplasmic protons and molecular oxygen to H_2O (1). In the process, the protein pumps out $2H^+$ for every electron, leading to the generation of PMF (**Figure 2*a***). The NDH-II complex is responsible for transferring two electrons from NADH, via an FAD cofactor, to the

membrane quinone pool (74) (**Figure 2*b***). Similarly, the SDH complex catalyzes the oxidation of succinate to fumarate and in so doing transfers two electrons to the quinone pool (92) (**Figure 2*c***). NDH-I is a large, multisubunit complex that contains a cytoplasmic NADH-binding domain with an FMN cofactor, several iron-sulfur cluster proteins, and a number of transmembrane proteins (23). NDH-I oxidizes NADH to NAD, transferring two electrons to the quinone pool and concomitantly pumping out four protons, thus contributing to the PMF (73) (**Figure 2*d***).

Because these systems are upregulated during aerobic growth under mild acid stress, a higher rate of proton export is expected under these conditions than under growth conditions at neutral

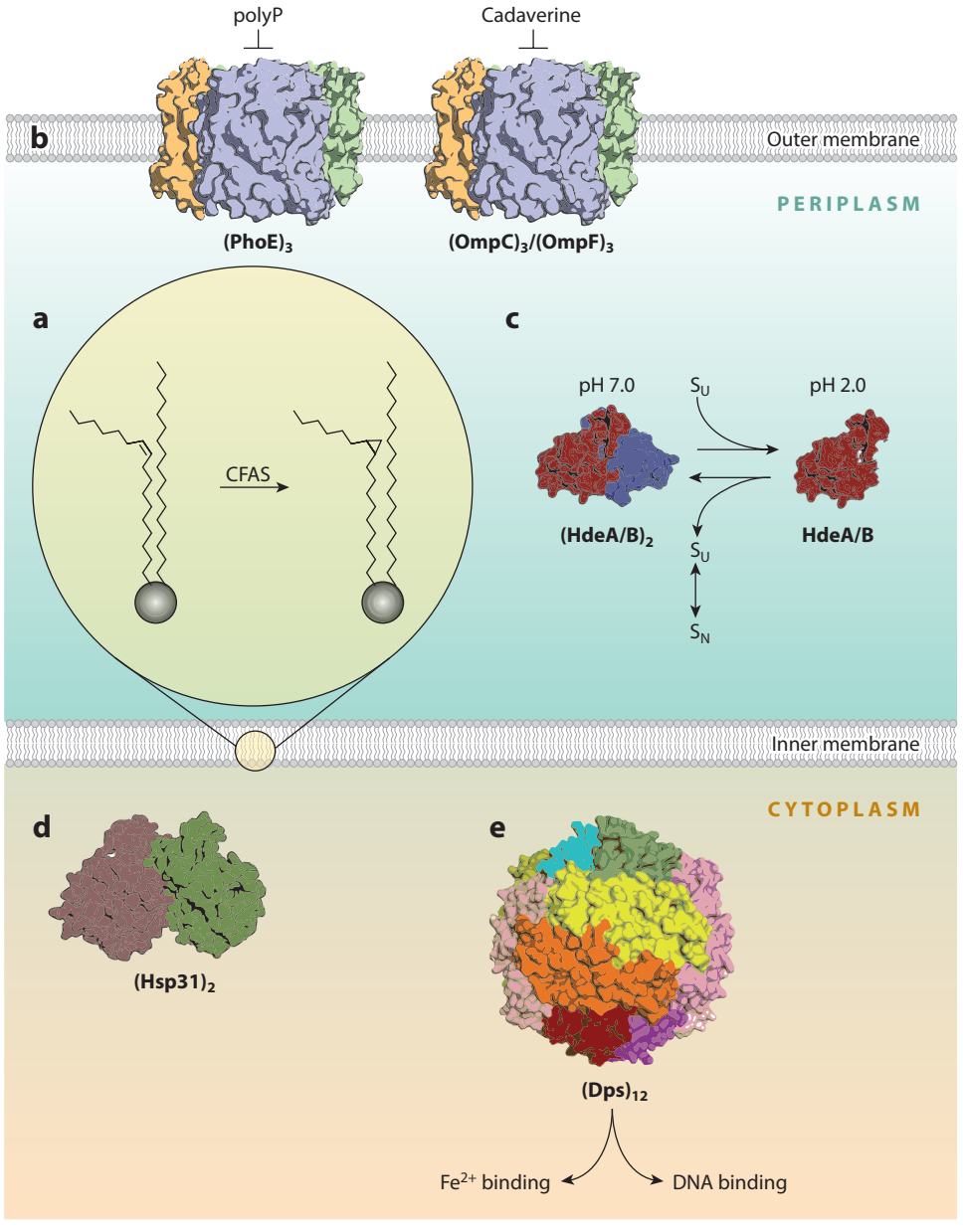

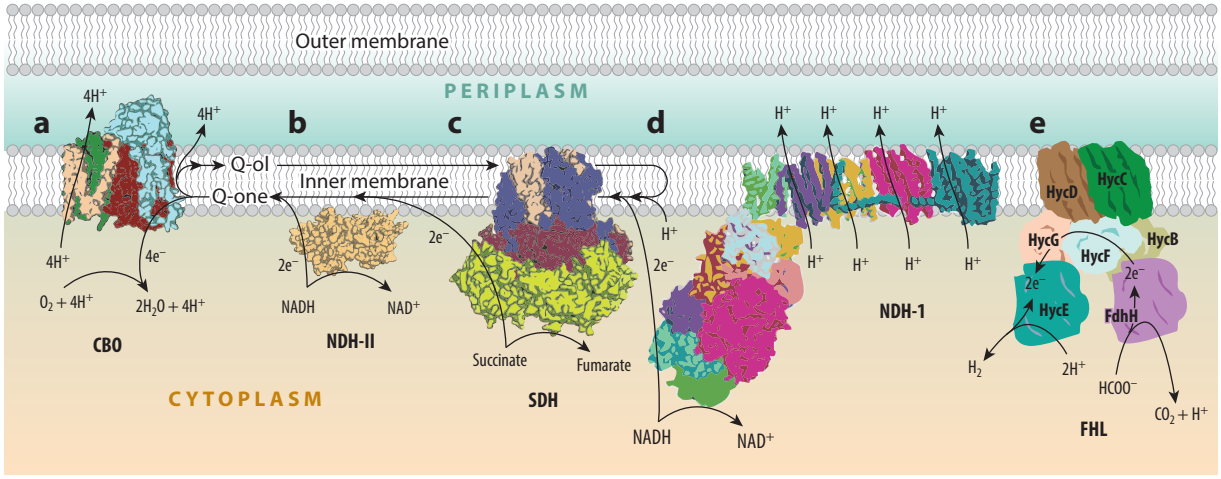

Figure 2

Metabolic responses to acid stress. Schematic illustration of the members of the oxidative electron transport chain that are implicated in proton efflux during mild acid stress under aerobic growth conditions (38, 58). (*a*) The cytochrome *bo* oxidase (CBO) complex reduces molecular oxygen to H_2O using electrons from the membrane quinone pool and in doing so exports cytoplasmic protons to generate the proton motive force (PMF) (1). (*b*) The NADH dehydrogenase II (NDH-II) complex transfers electrons to the quinone pool from NADH via an FAD cofactor (74). (*c*) The succinate dehydrogenase (SDH) complex transfers electrons to the quinone pool during oxidation of succinate to fumarate (92). (*d*) The NADH dehydrogenase I (NDH-I) complex contributes electrons from NADH to the quinone pool and contributes to PMF by directly pumping out protons (73). The redox cycling between the quinone (Q-one) and quinol (Q-ol) pools is shown schematically. (*e*) Schematic diagram of the formate hydrogen lyase (FHL) complex that couples oxidation of formic acid to CO_2 by formate dehydrogenase (FdhH) with the reduction of two H^+ to molecular hydrogen (H_2) by the hydrogenase-3 complex (HycBCDEFG) (62, 72).

pH (38, 58). This would enable the cell to actively counteract cytoplasmic pH drops by directly exporting protons.

PROTON-CONSUMING ACID RESISTANCE MECHANISMS

The basis of action of these types of acid resistance systems is the direct consumption of intracellular protons to counteract acid stress. Two major classes have been identified: the hydrogen-gas-producing formate hydrogen lyase (FHL) complex and the pyridoxal-5′-phosphate (PLP)-dependent amino acid decarboxylase AR systems.

PLP: pyridoxal-5′-phosphate

Figure 1

Physiological adaptations to acid stress. (*a*) The action of cyclopropane fatty acyl phospholipid synthase (CFAS) results in the addition of a methylene group to an unsaturated phospholipid tail (8, 14). (*b*) The trimeric outer membrane porin $(PhoE)_3$ (16) is blocked by polyphosphate anions (polyP) (68) and the $(OmpC)_3$ (6) and $(OmpF)_3$ (16) porins are blocked by cadaverine, the decarboxylation product of the inducible and constitutive lysine decarboxylases, during acid stress (19, 71). (*c*) Schematic of the functional cycle of the periplasmic acid-denatured chaperone HdeA/B (28). The protein is dimeric at neutral pH but dissociates into a partially unfolded monomer at pH 2.0 (80). The monomer binds to unfolded substrate (S_U) at pH 2.0, and the substrate is released and refolds to the native state S_N as the pH returns to neutral. (*d*) The cytoplasmic chaperone $(Hsp31)_2$ (65) functions as a holdase and stabilizes acid-unfolded client proteins during acid stress (61). (*e*) Dodecameric Dps forms a protein cage with a hollow interior that sequesters Fe^{2+} and reduces hydroxyl radical formation (9). The protein is also capable of protecting DNA by directly binding to and sequestering DNA in large Dps aggregates.

PLP-dependent amino acid decarboxylase: an enzyme that catalyzes the removal of the α-carbonyl group of an amino acid to generate CO2 and a decarboxylation product

Anaerobic growth under mild acidity induces the Ni^{2+}-dependent hydrogenase-3 complex (HycBCDEFG), which reduces protons to hydrogen gas (38, 62) (**Figure 2*e***). The electrons required to reduce H^+ are derived from the oxidation of formate by formate dehydrogenase-H, which together with hydrogenase-3 forms the FHL complex (**Figure 2*e***). The FHL complex converts formate to CO_2 and H_2 and is important for survival under anaerobic extreme acid stress.

Four distinct amino acid–dependent AR systems have been characterized, and each has two components: a cytoplasmic PLP-dependent decarboxylase that catalyzes a proton-dependent decarboxylation of a substrate amino acid to product and CO_2, and an inner membrane substrate/product antiporter that facilitates the continued operation of the system by exchanging external substrate for internal product (27). The AR systems are the glutamic acid–dependent acid resistance (GDAR) system, consisting of the homologous inducible glutamic acid decarboxylases GadA/GadB enzymes and the glutamate/γ-aminobutyric acid (GABA) antiporter GadC; the arginine-dependent acid resistance (ADAR) system, consisting of the inducible arginine decarboxylase AdiA and the arginine/agmatine antiporter AdiC; the lysine-dependent acid resistance (LDAR) system, consisting of the inducible lysine decarboxylase LdcI and the lysine/cadaverine

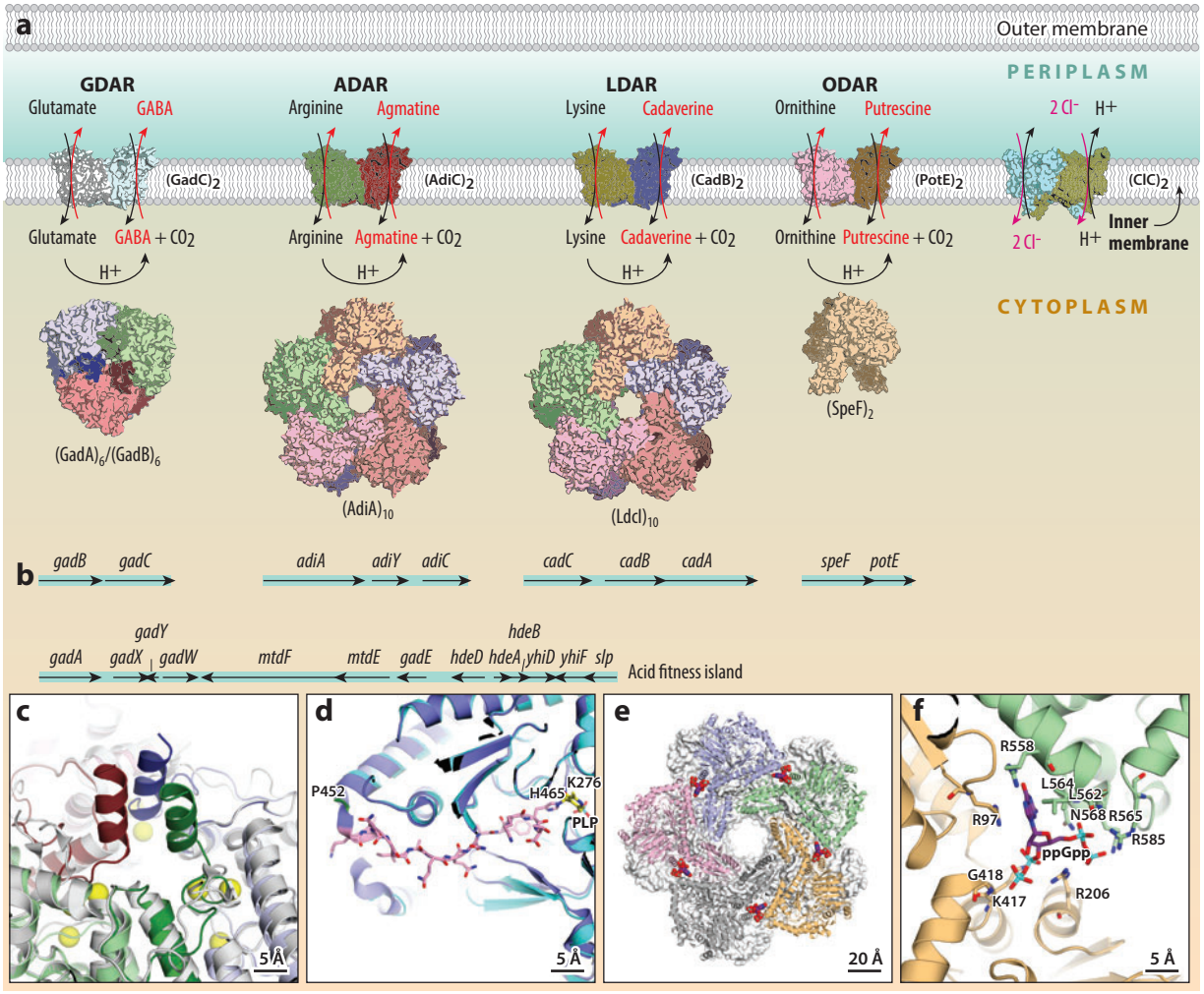

antiporter CadB; and the ornithine-dependent acid resistance (ODAR) system, consisting of the inducible ornithine decarboxylase SpeF and the ornithine/putrescine antiporter PotE (45) (**Figure 3*a***). The GDAR and ADAR systems provide robust protection against extreme acid stress (13, 53, 54) and enhance survival of cells exposed to SCFAs (36, 54, 60). The LDAR system operates most efficiently under mild acid stress conditions (27, 44), and the ODAR system is proposed to play a role under similar conditions (47).

The regulation of the AR systems is complex and our understanding of the various mechanisms for controlling gene expression is evolving (27, 94). The GDAR system is primarily induced upon entry into stationary phase (13, 17, 53) but is also activated during exponential growth in acidified media (12, 88). The *gadB* and *gadC* genes are cotranscribed as part of the *gadBC* operon (89) (**Figure 3*b***), and *gadA* is transcribed either alone or in combination with the downstream regulator protein *gadX* as part of the *gadAX* operon (86). Many of the GDAR genes, along with other stress response genes such as HdeA and HdeB, are found in an acid fitness island (AFI) (**Figure 3*b***), which is subject to extensive regulation (11, 32, 67, 85). The AFI genes, as well as other acid stress response genes such as *dps* and *cfa*, are under the control of the stationary-phase sigma factor RpoS (9, 14, 27) and contribute to the increased stress tolerance of stationary-phase cells. The ADAR system is induced maximally during growth under anaerobic, acidic (pH ~ 5.0) conditions in complex media (7, 59). *adiA*, the regulatory gene *adiY*, and the antiporter *adiC* are found clustered one after another on the chromosome; however, they are not thought to form an operon (**Figure 3*b***). The LDAR system is optimally induced under conditions of anaerobic growth at pH 5.5 in rich media with excess lysine (70). The *cadA* (coding for LdcI) and *cadB* genes are found together in the *cadBA* operon and these genes are regulated via the upstream *cadC* gene product (90) (**Figure 3*b***). CadC has an N-terminal ToxR-like DNA-binding domain, a single-spanning transmembrane helix, and a C-terminal periplasmic domain composed of two subdomains (24). CadC integrates *cadBA*

Antiporter: a membrane protein that catalyzes the transport of two substrates in opposite directions down their respective concentration gradients

GDAR: glutamic acid–dependent acid resistance system

ADAR: arginine-dependent acid resistance system

LDAR: lysine-dependent acid resistance system

ODAR: ornithine-dependent acid resistance system

Figure 3

Amino acid decarboxylases and inner membrane antiporters. (*a*) A schematic diagram illustrating the components of the amino acid decarboxylase acid resistance (AR) systems. The inner membrane glutamate/γ-aminobutyric acid (GABA) antiporter $(GadC)_2$ and the cytoplasmic glutamate decarboxylases $(GadA)_6/(GadB)_6$ (10, 20) constitute the glutamic acid–dependent acid resistance system (GDAR). The inner membrane arginine/agmatine antiporter $(AdiC)_2$ (30) and the cytoplasmic inducible arginine decarboxylase $(AdiA)_{10}$ (4) constitute the arginine-dependent acid resistance system (ADAR). The inner membrane lysine/cadaverine antiporter $(CadB)_2$ and the cytoplasmic inducible lysine decarboxylase $(LdcI)_{10}$ (44) constitute the lysine-dependent acid resistance system (LDAR). The ornithine/putrescine antiporter $(PotE)_2$ and the cytoplasmic inducible ornithine decarboxylase $(SpeF)_2$ constitute the ornithine-dependent acid resistance system (ODAR). The inner membrane chloride/proton antiporter $(ClC)_2$ (2, 21, 22) is involved in extreme acid stress resistance (27). For the four decarboxylase systems, the decarboxylation reaction is represented schematically: Substrate is decarboxylated in a proton-dependent manner to form product (*red*). The inner membrane antiporter then transports product to the periplasm (*red arrow*) in exchange for periplasmic substrate entering the cytoplasm (*black arrow*). For $(ClC)_2$, periplasmic Cl^- ions (*pink*) are exchanged (*pink arrows*) for cytoplasmic protons (*black arrows*). (*b*) Chromosomal organization of the AR genes and related regulatory genes; included are genes that compromise the acid fitness island (27, 57, 85). (*c*) The pH-dependent conformational change at the N terminus of GadB is shown. The structure of GadB at pH 7.6 (PDB ID: 1PMO) (10) is shown in gray, and superimposed on this is the structure of GadB at pH 4.6 (PDB ID: 1PMM) where each monomer is colored either red, pink, blue, light blue, dark green, or green. At low pH, the unstructured N terminus from each monomer forms a helix and the three adjacent helices form a triple-helical bundle that is stabilized by halide ions (*yellow spheres*) at the base of the N-terminal helices. The halide ions' positions are from Reference 37 (PDB ID: 2DGL, 2DGM). (*d*) At pH 4.6 (PDB ID: 1PMM; *cyan*), the C terminus of GadB is visible only until residue P452 (*green*); however, at pH 7.6 (PDB ID: 2DGK; *blue*) the C terminus, shown as pink sticks, becomes structured and blocks access to the active site. In addition, there is a unique aldamine bond between the penultimate histidine (H465) and the pyridoxal 5′-phosphate (PLP) cofactor (*yellow*) (37). (*e*) The stringent response alarmone ppGpp binds to the LdcI decamer (44). The top five monomers of the LdcI decamer are colored differently, the bottom five monomers are shown as surface representations, and the ppGpp molecules are shown as spheres. (*f*) Close-up view of one ppGpp-binding site at the interface between neighboring monomers in the LdcI decamer. Panels *c–f* were prepared using PyMOL (18).

induction via direct sensing of external pH through the periplasmic domain (24, 81) and indirect sensing of lysine levels via an interaction between the transmembrane helix and the lysine-specific permease, LysP (82). Finally, the *speF* and *potE* genes are located on an operon and are induced during growth at low pH (pH ~ 5.0); however, the regulation of these genes is not well understood (47).

PLP-Dependent Decarboxylases

The cytoplasmic decarboxylases GadA/B, AdiA, LdcI, and SpeF are Fold Type I PLP-dependent decarboxylases (**Figure 3*a***) and share a conserved PLP-binding domain that is involved in catalyzing the decarboxylation reaction (35, 75). GadA and GadB belong to the glutamate decarboxylase subclass and each has three domains: a short N-terminal stretch, a large domain that binds PLP, and a small domain (10). The paralogous AdiA, LdcI, and SpeF belong to the prokaryotic ornithine decarboxylase (pODC) subclass, which also includes the constitutive lysine decarboxylase (LdcC) and the constitutive ornithine decarboxylase (SpeC); however, these last two enzymes are not involved in acid stress resistance. Each pODC enzyme has five structural parts: an N-terminal Wing domain, a core domain composed of a short linker region, a PLP-binding subdomain (PLP-SD), subdomain four (SD4) [alternatively known as the aspartate aminotransferase (AAT)-like small domain], and a C-terminal domain (CTD) (4, 45). An important feature of the decarboxylases is oligomerization. At minimum, all the enzymes form homodimers and this is mediated primarily by the PLP-binding domain (43). Furthermore, GadA/GadB oligomerize to form hexamers (a trimer of dimers) (10), and AdiA (4) and LdcI (44) form star-shaped decamers (a pentamer of dimers) via interaction between the Wing domain and SD4 domains. SpeF is found predominantly in a dimeric form (45).

The decarboxylases also have optimal enzyme activities that are generally lower than neutral pH: between pH 3.7 and 3.8 for GadA/GadB (51, 76), between pH 4.9 and 5.2 for AdiA (7, 51), approximately pH 5.7 for LdcI (29, 70), and pH 7.0 for SpeF (5, 45). The efficiency of the AR systems to withstand extreme acid stress is correlated with the pH optima of the decarboxylases (GDAR > ADAR > LDAR $\gg$ ODAR) (27). The enzyme activity decreases sharply as the pH increases (37, 45), but because the pH optima range from ~pH 4 to pH 7, *E. coli* can mount a robust acid stress response due to the overlapping activities of the different AR systems (45). In addition, downregulation of decarboxylase activity as the pH increases may be an important factor in conserving cellular pools of amino acids and may prevent excessive alkalinization of the cytoplasm once the external acid stress has been neutralized.

Elucidation of the X-ray crystal structure of GadB at low (pH 4.6) and neutral (pH 7.6) pH values has shown that the enzyme undergoes a conformational change at its N terminus in response to changes in pH (10) (**Figure 3*c***). The first 14 N-terminal residues of the protein are largely unstructured at neutral pH but at low pH form an α-helix. The helices from three adjacent monomers combine to form a triple-helical bundle that projects outward from the surface of the structure, which is stabilized by binding to monovalent anions (Cl^-, Br^-, or I^-) at the base of the helix (37). The helical bundle increases the association of the protein with the inner membrane, and this is thought to increase the effectiveness of the enzyme as the proton concentration adjacent to the inner membrane is likely higher here than in the rest of the cell (10). Chloride ions are also effective in activating GadB and extending the activity of the enzyme over a wider range of pH values. At neutral pH, GadB activity is drastically reduced and this is accomplished in a unique fashion. The C-terminal 16 residues block the active site channel of the protein, and the penultimate H465 residue forms a unique covalent bond at the active site (37) (**Figure 3*d***). In the active enzyme there is an sp^2-hybridized bond between the PLP C4′ and the terminal nitrogen of K276, forming a Schiff base. However, at neutral pH there is an additional bond formed between

the distal ring nitrogen of H465 and PLP C4′, resulting in an sp^3-hybridized form known as an aldamine or geminal diamine that results in an inactive enzyme. When the pH decreases, the aldamine is lost and the C-terminal residues become unstructured, thus freeing up the active site.

AdiA activity is regulated primarily by a change in the oligomerization state of the enzyme (4, 45). At the pH of maximal activity (pH 5.2), the predominant species is the AdiA decamer, which dissociates into dimers with increasing pH (7). AdiA dimers are inactive at pH 5.2, but at pH 7.2 the decamers and dimers have similar activity; however, this activity is a small fraction of the maximal activity found at pH 5.2 (63). This suggests that increasing pH alone may also negatively regulate enzyme activity irrespective of the oligomeric state. The structure of AdiA has revealed that there are a large number of negatively charged surface residues, and it has been proposed that an increase in pH results in an electrostatic repulsion that enhances the decamer-to-dimer transition (4).

LdcI activity is regulated by two distinct mechanisms: oligomerization and the alarmone (p)ppGpp. The LdcI decamer is the predominant species at low and neutral pH and high enzyme concentrations, but the protein dissociates to form dimers at high pH (pH 8.0) and low salt concentrations (3, 44). This dissociation is not enhanced by electrostatic repulsion of negatively charged surface residues as is the case for AdiA. LdcI activity is strongly inhibited by the effector molecule of the stringent response (p)ppGpp, and this modified nucleotide binds at a unique site between neighboring dimers in the decamer (44) (**Figure 3*e*,*f***). (p)ppGpp is synthesized from ATP and GTP in response to nutritional limitation and other stresses and has multiple pleiotropic effects on RNA synthesis, protein synthesis, and gene regulation, resulting in a switch from exponential to stationary-phase growth (46). The inhibition of LdcI by (p)ppGpp provides cells with a rapid and reversible mechanism to regulate the decarboxylation of lysine under conditions when amino acids become limiting, thus enhancing cell survival. Furthermore, the paralogous LdcC, SpeF, and SpeC enzymes (but not AdiA) are similarly regulated by (p)ppGpp, suggesting that this is a common mechanism for modulating consumption of amino acids during stress and starvation conditions (45).

(p)ppGpp: the stringent response alarmone; a mixture of ppGpp (guanosine 3′, 5′-bis(diphosphate)) and pppGpp (guanosine 3′-diphosphate, 5′-triphosphate)

Stringent response: the starvation- and stress-induced shift from exponential to stationary-phase growth that is mediated by the alarmone (p)ppGpp

Inner Membrane Amino Acid Antiporters

The four inner membrane amino acid antiporters GadC, AdiC, CadB, and PotE belong to the amino acid/polyamine/organocation superfamily of membrane transporters (42). The antiporters, although sharing relatively low levels of sequence identity, have a common structural fold: They have 12 transmembrane helices, with the first 10 helices forming the protein core and with helices TM11 and TM12 involved in dimer formation (25, 30, 55). Among the 10 core helices, the first 5 (TM1–TM5) and the second 5 (TM6–TM10) are related by a pseudo-twofold rotational symmetry (**Figure 4*a*,*b***). This feature (a 5+5 inverted repeat) is conserved in a number of other transporter families, including the sodium-coupled symporters such as LeuT, BetP, and MhlP (25, 30, 49). In addition, the first helix in TM1 and TM6 is disrupted by a short loop region important for substrate binding and translocation. Each monomer in the protein dimer is capable of operating independently (25).

The recent elucidation of a number of high-resolution X-ray crystal structures of AdiC (25, 30, 31, 49) and GadC (55) has provided valuable insights into the mechanism of substrate binding and transport through the transporter pore. The transporters are proposed to cycle between two major conformations, periplasmic-open and cytoplasmic-open, each of which exposes a substrate-binding site to different faces of the membrane. Substrate binding leads to conformational changes and a transition through an occluded state where the substrate is buried in the transporter (**Figure 4*c***). Structures of *apo E. coli* AdiC (30) and *apo Salmonella enterica* serovar Typhimurium AdiC (95% identical to *E. coli* AdiC) (25) have been determined in the periplasmic-open conformation,

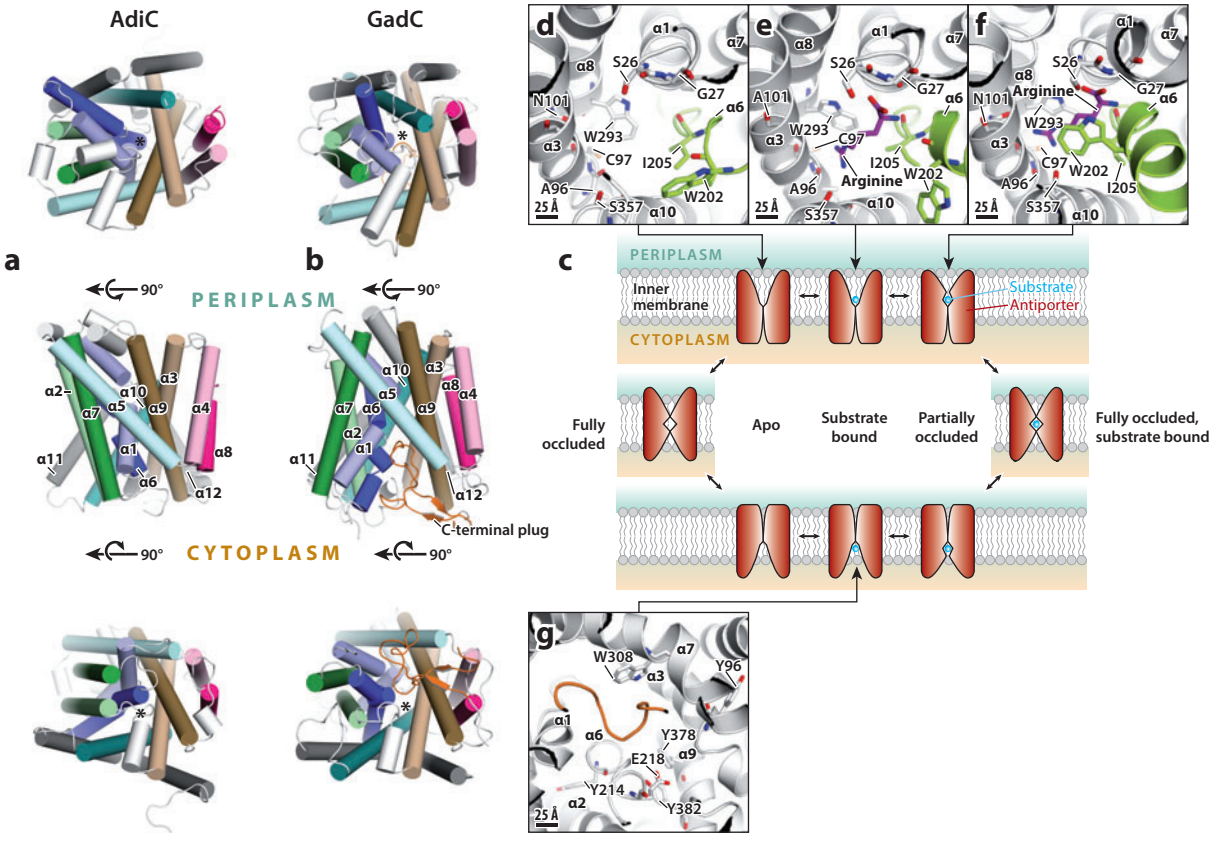

Figure 4

Escherichia coli inner membrane antiporters. A schematic of (*a*) an AdiC monomer (PDB ID: 3OB6) (49) and (*b*) a GadC monomer (PDB ID: 4DJI) (55) showing the 12 transmembrane helices. Helices α1–α5 are shown in a light color and the pseudosymmetry-related helices α6–α10 are shown in a corresponding darker color. The C-terminal plug of GadC is orange. Three views are shown: from the periplasmic face (*top*), from within the lipid bilayer (*middle*), and from the cytoplasmic face (*bottom*). The approximate position of the central pore in each transporter is indicated by an asterisk. (*c*) A schematic of the antiporter transport cycle based on Reference 49 is shown. In the *apo* state, the protein is open either to the periplasm or to the cytoplasm. Upon substrate binding from either periplasm or cytoplasm, the protein adopts a partially occluded state before undergoing conformational changes to a symmetrical, fully occluded, substrate-bound state. From the fully occluded state, the substrate is able to traverse the membrane and the cycle reverses to enable substrate release. (*d–f*) Periplasmic views of the arginine-binding pocket in AdiC. (*d*) View of the wild-type Apo form (PDB ID: 3LRB) (30). (*e*) View of the N101A mutant arginine-bound form (PDB ID: 3OB6) (49). (*f*) View of the N22A mutant partially occluded, arginine-bound form (PDB ID: 3L1L) (31). Residues involved in substrate binding are labeled, and helix α6, which undergoes significant movement upon formation of the substrate-bound and partially occluded states, is green. (*g*) Cytoplasmic view of the proposed GadC-binding pocket (PDB ID: 4DJI) (55). Residues implicated in substrate binding are labeled and the portion of the C-terminal plug occluding the binding site is orange. This figure was prepared using PyMOL (18).

whereas the structure of *E. coli* GadC was solved in a cytoplasmic-open conformation (55). Furthermore, two periplasm-facing structures of *E. coli* AdiC have been determined to be bound to arginine: an N101A mutant obtained in a substrate-bound open conformation (49) and an N22A mutant obtained in an occluded conformation (31).

The arginine-binding site in AdiC and the proposed translocation pathway have residues that show a high degree of conservation among related orthologs such as CadB and PotE (30). Arginine

binding is anchored by hydrogen-bonding interactions with the C_α amino and carboxyl groups (31) (**Figure 4*d–f***). The guanidinium group takes part in both hydrogen-bonding interactions and cation-π interactions with two tryptophan residues (W202 and W293). Three distinct gates have been proposed (with respect to the periplasm) to control binding and passage of arginine: a proximal gate (S26 and W202) in which binding of the substrate guanidinium group induces transition from the substrate-bound open conformation to the occluded conformation (49), a middle gate (W293), and a distal gate (Y93, E208, and Y365). Residues in the last two gates are thought to undergo rearrangements to accommodate substrate transport (31).

Completion of transport requires transition to the cytoplasmic-open conformation, and two models have been proposed. In both models, the transmembrane helices are grouped together into functional units: the bundle (or gate) domain (TMs 1, 2, 6, and 7) and the hash (or core) domain (TMs 3, 4, 8, and 9). TMs 5, 10, 11, and 12 do not undergo significant movement in either model. In the first model, the pseudosymmetry of the 5+5 inverted repeat of the core of the transporter constrains the movement of the protein, with both bundle and hash domains pivoting around the central pseudosymmetry axis (49). In the second model, the core domain (in addition to TM5 and TM10) remains fixed, whereas the gate domain undergoes large-scale rigid-body movements (55).

AdiC and GadC show a pH-dependent change in transport activity, with higher transport activities at lower pH values (25, 55). The pH dependence of different faces of the protein has been elegantly determined by making use of an AdiC active-site S26C mutant that is selectively inactivated on either side of the membrane by permeable or impermeable thiol-modifying agents (87). This technique showed that the extracellular surface of AdiC has a pH optimum between 3 and 4 and is lower than the optimum for the intracellular surface, which has a pH between 5 and 6. These values correspond relatively well with the known values of internal and external pH during extreme acid stress (91). AdiC is further constrained during its function under extreme acid stress, as the protein has to selectively transport singly charged arginine (Arg^+) (a minor species below pH 2.3) instead of the doubly protonated arginine (Arg^{2+}) to avoid a futile proton cycle (26, 87). AdiC binding to the Agm^{2+} analogue argininamide is approximately fivefold lower on the extracellular face than when it binds to Agm^+, indicating that a mechanism for selecting the correct substrate exists. Molecular dynamics simulations have suggested a role for E208 in regulating agmatine release during transport (96), but a detailed understanding of correct substrate selection is still incomplete. GadC shows a sharper change in pH-dependent transport activity compared with AdiC. At high pH values, the C-terminal plug (residues 477–511) blocks the transport pathway and prevents binding of the substrate (55) (**Figure 4*b*,*g***). Deletion of these residues results in an increase in activity of the enzyme at high pH and suggests that these residues may either become disordered or adopt a different conformation to allow substrate transport activity.

Mechanistic insights into the function of CadB and PotE are not as extensive, but mutational analysis of CadB has identified residues important for substrate transport (78, 79) that were subsequently shown to be important for AdiC activity (25, 30, 31). Recent modeling studies of CadB and PotE based on the AdiC structures have extended these findings (84).

THE ROLE OF CHLORIDE TRANSPORTERS IN EXTREME ACID RESISTANCE

Although GDAR and ADAR are the primary systems that operate under extreme acid stress, Iyer et al. (41) identified a critical role for the homodimeric bacterial chloride transporters (ClC) (**Figure 3*a***) under such conditions (2, 21, 22). The assumption under their model was that during extreme acid stress (external pH of 2–3, internal pH ~ 4.5), HCl would enter the cell in an

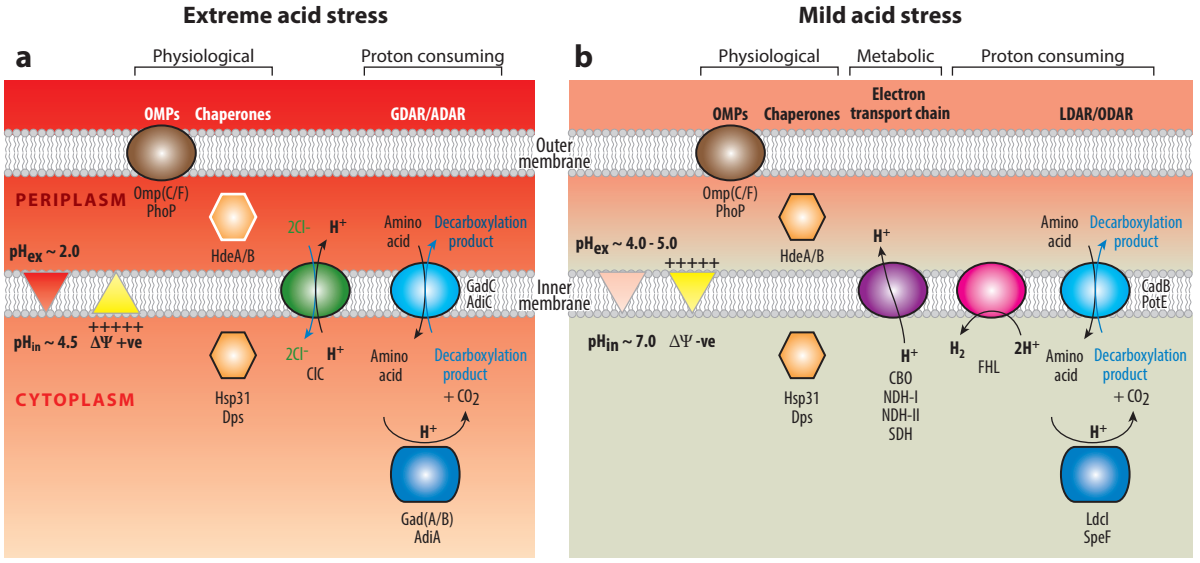

Figure 5

Global view of the *Escherichia coli* acid stress response. A schematic model showing the coordinated response of the cell to (*a*) extreme acid stress and (*b*) mild acid stress. The external pH (pH_{ex}) and internal pH (pH_{in}) under the two stress conditions are shown and the red triangle indicates the relative transmembrane proton gradient. Similarly, the yellow triangle indicates the direction of the transmembrane potential ($\Delta\Psi$), which is reversed under extreme acid stress conditions. The major physiological, metabolic, and proton-consuming systems thought to operate under each condition are illustrated.

uncharged state and subsequently dissociate into H^+ and Cl^- ions (41). The H^+ cation would be consumed by the GDAR and ADAR systems as described but the presence of the Cl^- anion could lead to hyperpolarization of the transmembrane potential ($\Delta\Psi$). Surprisingly, when radiometric measurements were made to determine the internal pH and $\Delta\Psi$ during extreme acid stress, it was found that *E. coli* cells reverse their $\Delta\Psi$ (66) (**Figure 5*a***). The inside-positive state is thought to result from a buildup of the more positively charged decarboxylation products (GABA and agmatine) that would necessarily accumulate in order to drive the exchange for fresh substrate via the antiporters GadC and AdiA. Furthermore, H^+ ions from the media are thought to enter the cell in a charged state and not as uncharged HCl. An inside-positive $\Delta\Psi$ could act to reduce the influx of protons via charge repulsion. Under these conditions, the ClC protein is thought to function as a H^+/Cl^- exchanger, driving the efflux of H^+ ions in exchange for Cl^- ions from the media; this is important in restoring the correct $\Delta\Psi$ (inside-negative) once the extreme acid stress condition has abated (27, 66).

CONCLUSION

For a neutralophile, *E. coli* is capable of mounting an effective resistance to an unexpectedly wide range of acid stress conditions thanks to the large number of acid stress response systems present in the cell. A summary of the systems that are active during extreme acid stress (**Figure 5*a***) and mild acid stress (**Figure 5*b***) is discussed. At a certain level, it is expected that all these systems must coordinate their response, which is currently poorly understood and is in need of further investigation. Some of these systems may be appropriate targets for the development of novel antimicrobials.

Transmembrane potential ($\Delta\Psi$): the electrochemical gradient across the inner membrane

SUMMARY POINTS

1. *E. coli* has three general types of active AR systems: physiological, metabolic, and proton-consuming.
2. The periplasm has physiological adaptations to acid stress, including membrane modifications and outer membrane porins that reduce proton influx, as well as pH-dependent chaperones.
3. Proton efflux can be coupled to metabolism via components of the electron transport chain (NDH-I, NDH-II, SDH, and cytochromes).
4. Under anaerobic growth conditions the FHL complex converts protons to H_2 gas.
5. Four proton-consuming amino acid–dependent acid resistance systems, ADAR, GDAR, LDAR, and ODAR, consist of a cytoplasmic decarboxylase and an inner membrane amino acid antiporter.
6. AdiA, GadA/B, LdcI, and SpeF decarboxylate substrate amino acids (arginine, glutamic acid, lysine, ornithine) in a proton-consuming reaction, which is catalyzed by PLP, to form the products CO_2 plus agmatine, GABA, cadaverine, and putrescine, respectively.
7. The inner membrane antiporters AdiC, GadC, CadB, and PotE catalyze the antiport of specific substrate/product pairs (arginine/agmatine, glutamic acid/GABA, lysine/cadaverine, and ornithine/putrescine).
8. ADAR and GDAR provide protection against extreme acid resistance. LDAR provides protection against mild acid resistance, and the regulation of this protein is linked to the stringent response via (p)ppGpp.

DISCLOSURE STATEMENT

The authors are not aware of any affiliations, memberships, funding, or financial holdings that might be perceived as affecting the objectivity of this review.

ACKNOWLEDGMENTS

U.K. is the recipient of a Canadian Institutes of Health Research Postdoctoral Fellowship, a National Sciences and Engineering Research Council of Canada Postgraduate Scholarship, a CIHR Strategic Training Program in the Structural Biology of Membrane Proteins Linked to Disease Scholarship, and a University of Toronto Open Fellowship. This work was supported by a grant from the Canadian Institutes of Health Research (MOP-67210) to W.A.H.

LITERATURE CITED

1. Abramson J, Riistama S, Larsson G, Jasaitis A, Svensson-Ek M, et al. 2000. The structure of the ubiquinol oxidase from *Escherichia coli* and its ubiquinone binding site. *Nat. Struct. Biol.* 7:910–17
2. Accardi A, Walden M, Nguitragool W, Jayaram H, Williams C, Miller C. 2005. Separate ion pathways in a Cl^-/H^+ exchanger. *J. Gen. Physiol.* 126:563–70
3. Alexopoulos E, Kanjee U, Snider J, Houry WA, Pai EF. 2008. Crystallization and preliminary X-ray analysis of the inducible lysine decarboxylase from *Escherichia coli*. *Acta Crystallogr. F* 64:700–6
4. Andrell J, Hicks MG, Palmer T, Carpenter EP, Iwata S, Maher MJ. 2009. Crystal structure of the acid-induced arginine decarboxylase from *Escherichia coli*: Reversible decamer assembly controls enzyme activity. *Biochemistry* 48:3915–27

5. Applebaum D, Sabo DL, Fischer EH, Morris DR. 1975. Biodegradative ornithine decarboxylase of *Escherichia coli*. Purification, properties, and pyridoxal 5′-phosphate binding site. *Biochemistry* 14:3675–81
6. Basle A, Rummel G, Storici P, Rosenbusch JP, Schirmer T. 2006. Crystal structure of osmoporin OmpC from *E. coli* at 2.0 Å. *J. Mol. Biol.* 362:933–42
7. Blethen SL, Boeker EA, Snell EE. 1968. Arginine decarboxylase from *Escherichia coli*. I. Purification and specificity for substrates and coenzyme. *J. Biol. Chem.* 243:1671–77
8. Brown JL, Ross T, McMeekin TA, Nichols PD. 1997. Acid habituation of *Escherichia coli* and the potential role of cyclopropane fatty acids in low pH tolerance. *Int. J. Food Microbiol.* 37:163–73
9. Calhoun LN, Kwon YM. 2011. Structure, function and regulation of the DNA-binding protein Dps and its role in acid and oxidative stress resistance in *Escherichia coli*: a review. *J. Appl. Microbiol.* 110:375–86
10. **Capitani G, De Biase D, Aurizi C, Gut H, Bossa F, Grutter MG. 2003. Crystal structure and functional analysis of *Escherichia coli* glutamate decarboxylase. *EMBO J.* 22:4027–37**
11. Castanie-Cornet MP, Cam K, Bastiat B, Cros A, Bordes P, Gutierrez C. 2010. Acid stress response in *Escherichia coli*: mechanism of regulation of *gadA* transcription by RcsB and GadE. *Nucleic Acids Res.* 38:3546–54
12. Castanie-Cornet MP, Foster JW. 2001. *Escherichia coli* acid resistance: cAMP receptor protein and a 20 bp *cis*-acting sequence control pH and stationary phase expression of the *gadA* and *gadBC* glutamate decarboxylase genes. *Microbiology* 147:709–15
13. Castanie-Cornet MP, Penfound TA, Smith D, Elliott JF, Foster JW. 1999. Control of acid resistance in *Escherichia coli*. *J. Bacteriol.* 181:3525–35
14. Chang YY, Cronan JE Jr. 1999. Membrane cyclopropane fatty acid content is a major factor in acid resistance of *Escherichia coli*. *Mol. Microbiol.* 33:249–59
15. Choi SH, Baumler DJ, Kaspar CW. 2000. Contribution of *dps* to acid stress tolerance and oxidative stress tolerance in *Escherichia coli* O157:H7. *Appl. Environ. Microbiol.* 66:3911–16
16. Cowan SW, Schirmer T, Rummel G, Steiert M, Ghosh R, et al. 1992. Crystal structures explain functional properties of two *E. coli* porins. *Nature* 358:727–33
17. De Biase D, Tramonti A, Bossa F, Visca P. 1999. The response to stationary-phase stress conditions in *Escherichia coli*: role and regulation of the glutamic acid decarboxylase system. *Mol. Microbiol.* 32:1198–211
18. DeLano WL. 2002. *The PyMOL Molecular Graphics System*. Palo Alto, CA: DeLano Sci.
19. delaVega AL, Delcour AH. 1995. Cadaverine induces closing of *E. coli* porins. *EMBO J.* 14:6058–65
20. Dutyshev DI, Darii EL, Fomenkova NP, Pechik IV, Polyakov KM, et al. 2005. Structure of *Escherichia coli* glutamate decarboxylase (GADα) in complex with glutarate at 2.05 Å resolution. *Acta Crystallogr. D* 61:230–35
21. Dutzler R, Campbell EB, Cadene M, Chait BT, MacKinnon R. 2002. X-ray structure of a ClC chloride channel at 3.0 Å reveals the molecular basis of anion selectivity. *Nature* 415:287–94
22. Dutzler R, Campbell EB, MacKinnon R. 2003. Gating the selectivity filter in ClC chloride channels. *Science* 300:108–12
23. Efremov RG, Baradaran R, Sazanov LA. 2010. The architecture of respiratory complex I. *Nature* 465:441–45
24. Eichinger A, Haneburger I, Koller C, Jung K, Skerra A. 2011. Crystal structure of the sensory domain of *Escherichia coli* CadC, a member of the ToxR-like protein family. *Protein Sci.* 20:656–69
25. **Fang Y, Jayaram H, Shane T, Kolmakova-Partensky L, Wu F, et al. 2009. Structure of a prokaryotic virtual proton pump at 3.2 A resolution. *Nature* 460:1040–43**
26. Fang Y, Kolmakova-Partensky L, Miller C. 2007. A bacterial arginine-agmatine exchange transporter involved in extreme acid resistance. *J. Biol. Chem.* 282:176–82
27. Foster JW. 2004. *Escherichia coli* acid resistance: tales of an amateur acidophile. *Nat. Rev. Microbiol.* 2:898–907
28. Gajiwala KS, Burley SK. 2000. HDEA, a periplasmic protein that supports acid resistance in pathogenic enteric bacteria. *J. Mol. Biol.* 295:605–12
29. Gale EF, Epps HM. 1944. Studies on bacterial amino-acid decarboxylases: 1. *l*(+)-lysine decarboxylase. *Biochem. J.* 38:232–42
30. **Gao X, Lu F, Zhou L, Dang S, Sun L, et al. 2009. Structure and mechanism of an amino acid antiporter. *Science* 324:1565–68**

10. Determined the X-ray crystal structure of GadB and observed the pH-dependent formation of an N-terminal helical bundle.

25. Determined the X-ray crystal structure of AdiC and proposed that this protein functions as a "virtual proton pump" via selectively importing singly charged arginine (1+) and exporting agmatine (2+) during extreme acid stress.

30. Determined the X-ray crystal structure of AdiC and proposed a substrate translocation mechanism that relies on the '5+5' inverted repeat structure of the protein monomer.

31. Gao X, Zhou L, Jiao X, Lu F, Yan C, et al. 2010. Mechanism of substrate recognition and transport by an amino acid antiporter. *Nature* 463:828–32
32. Gong S, Ma Z, Foster JW. 2004. The Era-like GTPase TrmE conditionally activates *gadE* and glutamate-dependent acid resistance in *Escherichia coli*. *Mol. Microbiol.* 54:948–61
33. Gorden J, Small PL. 1993. Acid resistance in enteric bacteria. *Infect. Immun.* 61:364–67
34. Grant RA, Filman DJ, Finkel SE, Kolter R, Hogle JM. 1998. The crystal structure of Dps, a ferritin homolog that binds and protects DNA. *Nat. Struct. Biol.* 5:294–303
35. Grishin NV, Phillips MA, Goldsmith EJ. 1995. Modeling of the spatial structure of eukaryotic ornithine decarboxylases. *Protein Sci.* 4:1291–304
36. Guilfoyle DE, Hirshfield IN. 1996. The survival benefit of short-chain organic acids and the inducible arginine and lysine decarboxylase genes for *Escherichia coli*. *Lett. Appl. Microbiol.* 22:393–96
37. Gut H, Pennacchietti E, John RA, Bossa F, Capitani G, et al. 2006. *Escherichia coli* acid resistance: pH-sensing, activation by chloride and autoinhibition in GadB. *EMBO J.* 25:2643–51
38. Hayes ET, Wilks JC, Sanfilippo P, Yohannes E, Tate DP, et al. 2006. Oxygen limitation modulates pH regulation of catabolism and hydrogenases, multidrug transporters, and envelope composition in *Escherichia coli* K-12. *BMC Microbiol.* 6:89
39. Hobbs EC, Astarita JL, Storz G. 2010. Small RNAs and small proteins involved in resistance to cell envelope stress and acid shock in *Escherichia coli*: analysis of a bar-coded mutant collection. *J. Bacteriol.* 192:59–67
40. Houry WA. 2001. Chaperone-assisted protein folding in the cell cytoplasm. *Curr. Protein Pept. Sci.* 2:227–44
41. Iyer R, Iverson TM, Accardi A, Miller C. 2002. A biological role for prokaryotic ClC chloride channels. *Nature* 419:715–18
42. Jack DL, Paulsen IT, Saier MH. 2000. The amino acid/polyamine/organocation (APC) superfamily of transporters specific for amino acids, polyamines and organocations. *Microbiology* 146(Pt. 8):1797–814
43. Käck H, Sandmark J, Gibson K, Schneider G, Lindqvist Y. 1999. Crystal structure of diaminopelargonic acid synthase: evolutionary relationships between pyridoxal-5′-phosphate-dependent enzymes. *J. Mol. Biol.* 291:857–76
44. Kanjee U, Gutsche I, Alexopoulos E, Zhao B, Thibault G, et al. 2011. Linking the bacterial acid stress and stringent responses: the structure of the inducible lysine decarboxylase. *EMBO J.* 30:931–44
45. Kanjee U, Gutsche I, Ramachandran S, Houry W. 2011. The enzymatic activities of the *Escherichia coli* basic aliphatic amino acid decarboxylases exhibit a pH zone of inhibition. *Biochemistry* 50:9388–98
46. Kanjee U, Ogata K, Houry WA. 2012. Direct binding targets of the stringent response alarmone (p)ppGpp. *Mol. Microbiol.* 85:1029–43
47. Kashiwagi K, Suzuki T, Suzuki F, Furuchi T, Kobayashi H, Igarashi K. 1991. Coexistence of the genes for putrescine transport protein and ornithine decarboxylase at 16 min on *Escherichia coli* chromosome. *J. Biol. Chem.* 266:20922–27
48. Kern R, Malki A, Abdallah J, Tagourti J, Richarme G. 2007. *Escherichia coli* HdeB is an acid stress chaperone. *J. Bacteriol.* 189:603–10
49. Kowalczyk L, Ratera M, Paladino A, Bartoccioni P, Errasti-Murugarren E, et al. 2011. Molecular basis of substrate-induced permeation by an amino acid antiporter. *Proc. Natl. Acad. Sci. USA* 108:3935–40
50. Krulwich TA, Sachs G, Padan E. 2011. Molecular aspects of bacterial pH sensing and homeostasis. *Nat. Rev. Microbiol.* 9:330–43
51. Lawson A, Quinn AG. 1967. Studies on amino acid decarboxylases in *Escherichia coli*. *Biochem. J.* 105:483–90
52. Lee J, Page R, Garcia-Contreras R, Palermino JM, Zhang XS, et al. 2007. Structure and function of the *Escherichia coli* protein YmgB: a protein critical for biofilm formation and acid resistance. *J. Mol. Biol.* 373:11–26
53. Lin J, Lee IS, Frey J, Slonczewski JL, Foster JW. 1995. Comparative analysis of extreme acid survival in *Salmonella typhimurium*, *Shigella flexneri*, and *Escherichia coli*. *J. Bacteriol.* 177:4097–104
54. Lin J, Smith MP, Chapin KC, Baik HS, Bennett GN, Foster JW. 1996. Mechanisms of acid resistance in enterohemorrhagic *Escherichia coli*. *Appl. Environ. Microbiol.* 62:3094–100

44. Determined the X-ray crystal structure of LdcI and showed novel regulation of this enzyme via the stringent response alarmone (p)ppGpp.

45. Demonstrated a zone of inhibition of *E. coli* amino acid decarboxylases.

55. Determined the X-ray crystal structure of GadC in an inward-facing conformation and discovered a novel C-terminal plug that regulates transporter activity in a pH-dependent manner.

55. Ma D, Lu P, Yan C, Fan C, Yin P, et al. 2012. Structure and mechanism of a glutamate-GABA antiporter. *Nature* 483:632–36

56. Marcus EA, Moshfegh AP, Sachs G, Scott DR. 2005. The periplasmic α-carbonic anhydrase activity of *Helicobacter pylori* is essential for acid acclimation. *J. Bacteriol.* 187:729–38
57. Mates AK, Sayed AK, Foster JW. 2007. Products of the *Escherichia coli* acid fitness island attenuate metabolite stress at extremely low pH and mediate a cell density-dependent acid resistance. *J. Bacteriol.* 189:2759–68
58. Maurer LM, Yohannes E, Bondurant SS, Radmacher M, Slonczewski JL. 2005. pH regulates genes for flagellar motility, catabolism, and oxidative stress in *Escherichia coli* K-12. *J. Bacteriol.* 187:304–19
59. Melnykovych G, Snell EE. 1958. Nutritional requirements for the formation of arginine decarboxylase in *Escherichia coli*. *J. Bacteriol.* 76:518–23
60. Moreau PL. 2007. The lysine decarboxylase CadA protects *Escherichia coli* starved of phosphate against fermentation acids. *J. Bacteriol.* 189:2249–61
61. Mujacic M, Baneyx F. 2007. Chaperone Hsp31 contributes to acid resistance in stationary-phase *Escherichia coli*. *Appl. Environ. Microbiol.* 73:1014–18
62. Noguchi K, Riggins DP, Eldahan KC, Kitko RD, Slonczewski JL. 2010. Hydrogenase-3 contributes to anaerobic acid resistance of *Escherichia coli*. *PLoS One* 5:e10132
63. Nowak S, Boeker EA. 1981. The inducible arginine decarboxylase of *Escherichia coli* B: activity of the dimer and the decamer. *Arch. Biochem. Biophys.* 207:110–16
64. Peterson WL, Mackowiak PA, Barnett CC, Marling-Cason M, Haley ML. 1989. The human gastric bactericidal barrier: mechanisms of action, relative antibacterial activity, and dietary influences. *J. Infect. Dis.* 159:979–83
65. Quigley PM, Korotkov K, Baneyx F, Hol WG. 2004. A new native EcHsp31 structure suggests a key role of structural flexibility for chaperone function. *Protein Sci.* 13:269–77
66. Richard H, Foster JW. 2004. *Escherichia coli* glutamate- and arginine-dependent acid resistance systems increase internal pH and reverse transmembrane potential. *J. Bacteriol.* 186:6032–41
67. Richard H, Foster JW. 2007. Sodium regulates *Escherichia coli* acid resistance, and influences GadX- and GadW-dependent activation of *gadE*. *Microbiology* 153:3154–61
68. Rowbury RJ, Goodson M, Wallace AD. 1992. The PhoE porin and transmission of the chemical stimulus for induction of acid resistance (acid habituation) in *Escherichia coli*. *J. Appl. Bacteriol.* 72:233–43
69. Ruiz C, McMurry LM, Levy SB. 2008. Role of the multidrug resistance regulator MarA in global regulation of the hdeAB acid resistance operon in *Escherichia coli*. *J. Bacteriol.* 190:1290–97
70. Sabo DL, Boeker EA, Byers B, Waron H, Fischer EH. 1974. Purification and physical properties of inducible *Escherichia coli* lysine decarboxylase. *Biochemistry* 13:662–70
71. Samartzidou H, Mehrazin M, Xu Z, Benedik MJ, Delcour AH. 2003. Cadaverine inhibition of porin plays a role in cell survival at acidic pH. *J. Bacteriol.* 185:13–19
72. Sauter M, Bohm R, Bock A. 1992. Mutational analysis of the operon (*hyc*) determining hydrogenase 3 formation in *Escherichia coli*. *Mol. Microbiol.* 6:1523–32
73. Sazanov LA. 2007. Respiratory complex I: mechanistic and structural insights provided by the crystal structure of the hydrophilic domain. *Biochemistry* 46:2275–88
74. Schmid R, Gerloff DL. 2004. Functional properties of the alternative NADH:ubiquinone oxidoreductase from *E. coli* through comparative 3-D modelling. *FEBS Lett.* 578:163–68
75. Schneider G, Käck H, Lindqvist Y. 2000. The manifold of vitamin B6 dependent enzymes. *Structure* 8:R1–6
76. Shukuya R, Schwert GW. 1960. Glutamic acid decarboxylase. I. Isolation procedures and properties of the enzyme. *J. Biol. Chem.* 235:1649–52
77. Slonczewski JL, Fujisawa M, Dopson M, Krulwich TA. 2009. Cytoplasmic pH measurement and homeostasis in bacteria and archaea. *Adv. Microb. Physiol.* 55:1–79
78. Soksawatmaekhin W, Kuraishi A, Sakata K, Kashiwagi K, Igarashi K. 2004. Excretion and uptake of cadaverine by CadB and its physiological functions in *Escherichia coli*. *Mol. Microbiol.* 51:1401–12
79. Soksawatmaekhin W, Uemura T, Fukiwake N, Kashiwagi K, Igarashi K. 2006. Identification of the cadaverine recognition site on the cadaverine-lysine antiporter CadB. *J. Biol. Chem.* 281:29213–20

80. Tapley TL, Franzmann TM, Chakraborty S, Jakob U, Bardwell JC. 2010. Protein refolding by pH-triggered chaperone binding and release. *Proc. Natl. Acad. Sci. USA* 107:1071–76
81. Tetsch L, Koller C, Donhofer A, Jung K. 2011. Detection and function of an intramolecular disulfide bond in the pH-responsive CadC of *Escherichia coli*. *BMC Microbiol.* 11:74
82. Tetsch L, Koller C, Haneburger I, Jung K. 2007. The membrane-integrated transcriptional activator CadC of *Escherichia coli* senses lysine indirectly via the interaction with the lysine permease LysP. *Mol. Microbiol.* 67:570–83
83. Texter EC Jr, Chou CC, Laurete HC, Vantrappen GR, eds. 1968. *Physiology of the Gastrointestinal Tract*. St. Louis, MO: C.V. Mosby Co. 262 pp.
84. Tomitori H, Kashiwagi K, Igarashi K. 2012. Structure and function of polyamine-amino acid antiporters CadB and PotE in *Escherichia coli*. *Amino Acids* 42:733–40
85. Tramonti A, De Canio M, De Biase D. 2008. GadX/GadW-dependent regulation of the *Escherichia coli* acid fitness island: transcriptional control at the *gadY-gadW* divergent promoters and identification of four novel 42 bp GadX/GadW-specific binding sites. *Mol. Microbiol.* 70:965–82
86. Tramonti A, Visca P, De Canio M, Falconi M, De Biase D. 2002. Functional characterization and regulation of *gadX*, a gene encoding an AraC/XylS-like transcriptional activator of the *Escherichia coli* glutamic acid decarboxylase system. *J. Bacteriol.* 184:2603–13
87. Tsai MF, Fang Y, Miller C. 2012. Sided functions of an arginine-agmatine antiporter oriented in liposomes. *Biochemistry* 51:1577–85
88. Tucker DL, Tucker N, Conway T. 2002. Gene expression profiling of the pH response in *Escherichia coli*. *J. Bacteriol.* 184:6551–58
89. Waterman SR, Small PL. 1996. Identification of σ^S-dependent genes associated with the stationary-phase acid-resistance phenotype of *Shigella flexneri*. *Mol. Microbiol.* 21:925–40
90. Watson N, Dunyak DS, Rosey EL, Slonczewski JL, Olson ER. 1992. Identification of elements involved in transcriptional regulation of the *Escherichia coli cad* operon by external pH. *J. Bacteriol.* 174:530–40
91. Wilks JC, Slonczewski JL. 2007. pH of the cytoplasm and periplasm of *Escherichia coli*: rapid measurement by green fluorescent protein fluorimetry. *J. Bacteriol.* 189:5601–7
92. Yankovskaya V, Horsefield R, Tornroth S, Luna-Chavez C, Miyoshi H, et al. 2003. Architecture of succinate dehydrogenase and reactive oxygen species generation. *Science* 299:700–4
93. Yuk HG, Marshall DL. 2004. Adaptation of *Escherichia coli* O157:H7 to pH alters membrane lipid composition, verotoxin secretion, and resistance to simulated gastric fluid acid. *Appl. Environ. Microbiol.* 70:3500–5
94. Zhao B, Houry WA. 2010. Acid stress response in enteropathogenic gammaproteobacteria: an aptitude for survival. *Biochem. Cell Biol.* 88:301–14
95. Zhao G, Ceci P, Ilari A, Giangiacomo L, Laue TM, et al. 2002. Iron and hydrogen peroxide detoxification properties of DNA-binding protein from starved cells. A ferritin-like DNA-binding protein of *Escherichia coli*. *J. Biol. Chem.* 277:27689–96
96. Zomot E, Bahar I. 2011. Protonation of glutamate-208 induces the release of agmatine in an outward-facing conformation of arginine/agmatine antiporter. *J. Biol. Chem.* 286:19693–701

Annual Review of Microbiology

Volume 67, 2013

Contents

Index

Errata

An online log of corrections to *Annual Review of Microbiology* articles may be found at http://micro.annualreviews.org/